Core-level magnetic-circular-dichroism study of an Fe single crystal, Fe-Pt alloys, and an Fe/Pt multilayer

T. Koide and T. Shidara
Photon Factory, National Laboratory for High Energy Physics, Tsukuba, Ibaraki 305, Japan

K. Yamaguchi* and A. Fujimori
Department of Physics, University of Tokyo, Bunkyo-ku, Tokyo 113, Japan

H. Fukutani
Institute of Physics, University of Tsukuba, Tsukuba, Ibaraki 305, Japan

N. Nakajima
Department of Physics, Tokyo Institute of Technology, Meguro-ku, Tokyo 152, Japan

T. Sugimoto†
College of Science and Technology, Nihon University, Funabashi, Chiba 274, Japan

T. Katayama and Y. Suzuki‡
Electrotechnical Laboratory, Tsukuba, Ibaraki 305, Japan
(Received 11 October 1994; revised manuscript received 5 June 1995)

We have studied the local magnetic states of a single-crystalline Fe film, annealed and as-deposited Fe-Pt alloy films, and an Fe/Pt multilayer by magnetic circular dichroism (MCD) in core-level absorption. The MCD spectra around the Fe $M_{2,3}$ edges unambiguously reveal an enhanced $3d$ orbital moment in the alloys and multilayer relative to that in Fe metal. MCD signals were also observed at the Pt $N_{6,7}$ and O_2 edges in the alloys and multilayer, showing induced magnetic moments on Pt atoms. A comparison of the MCD spectral pattern at the Pt $N_{6,7}$ edges with that at the Fe $M_{2,3}$ and Pt $O_{2,3}$ edges gives clear evidence that the induced Pt moments are aligned parallel to the Fe moments. Fine MCD features observed at the Pt $N_{6,7}$ edges indicate that the Pt $5d$ partial density of states just above the Fermi level is higher for the majority-spin states than for the minority-spin states.

The magnetic and magneto-optical properties of (Fe,Co)/(Pt,Pd) multilayers have recently attracted much attention in relation to magnetic data-storage applications. The favorable properties that make these systems promising candidates for next-generation high-density magneto-optical recording media include their spontaneous perpendicular magnetization, large Kerr rotations at short wavelengths in the visible and ultraviolet regions, and high oxidation and corrosion resistance.[1,2] The correlation and underlying mechanism of these phenomena have been the subjects of investigations from fundamental points of view. Studies of the magnetic and electronic states of (Fe,Co)/(Pt,Pd) binary alloys, which are closely related to the multilayers, are also of interest and importance. An understanding of the magnetism of these alloys will provide valuable clues for a better understanding of the magnetic properties of multilayers. A number of studies have been conducted for the (Fe,Co)/(Pt,Pd) multilayers and alloys using various experimental techniques.[1–6] Theoretical investigations, mainly based on spin-polarized band-structure calculations, have also been performed.[7–9] Nevertheless, the nature of the magnetism of the (Fe,Co)/(Pt,Pd) systems is still controversial.

Magnetic circular dichroism (MCD) in core-level absorption[10–12] has the advantages of element specificity and site selectivity, because the core-level MCD process involves optical transitions in which the initial states are well localized and have well-defined angular momenta. These favorable features of the core-level MCD provide a powerful tool for probing the magnetic and electronic states of magnetic substances, particularly those of multicomponent systems, such as magnetic alloys and multilayers as well as compounds. Several core-level MCD studies have very recently been reported for (Fe,Co)/(Pt,Pd) systems.[13–16] Most of the studies were carried out either at the core edges of only one constituent or at the core edges which involve final states indirectly related to the magnetism. However, for these binary systems, it would be highly desirable to measure the MCD at ''magnetism-related'' core edges of both constituents using the same experimental setup, since Pt or Pd, as well as Fe or Co, are expected to be responsible for the magnetism.

In this paper we report on a core-level MCD study of annealed and as-deposited Fe-Pt alloy films and an Fe/Pt multilayer in the 40–80-eV range. This energy region covers the Pt $N_{6,7}$ ($4f_{5/2,7/2} \rightarrow 5d$) and $O_{2,3}$ ($5p_{1/2,3/2} \rightarrow 5d$) core edges as well as the Fe $M_{2,3}$ ($3p_{1/2,3/2} \rightarrow 3d$) edges. For a reference, the MCD spectrum of a single-crystalline Fe film is also presented.

The annealed and as-deposited $Fe_{51}Pt_{49}$ alloy films were prepared onto heated (~380 °C) and water-cooled (~20 °C) quartz substrates, respectively, by an rf cosputtering method.[3,4] An Fe(4.7 Å)/Pt(18.5 Å) multilayer (i.e., 80 bi-

layer) sample was deposited onto a rotating water-cooled (~20 °C) glass substrate by the rf sputtering method with two targets.[2] To prevent the sample surface from oxidation, the top layer of the multilayer was of Pt (18.5 Å) and the alloy films were overcoated with a 10-Å-thick Pt layer. It was confirmed by x-ray diffraction that the as-deposited alloy film had a face-centered-cubic (fcc) structure (a disordered phase) and the annealed one a face-centered-tetragonal (fct) structure (presumably an ordered phase). The multilayer was found to have a periodic structure along the normal to the film plane. A 1000-Å-thick body-centered-cubic (bcc) Fe(100) film was made by a molecular-beam-epitaxy (MBE) technique on a (100) cleaved surface of a MgO single-crystal substrate with 2000-Å-thick fcc Ag(100) and 2000-Å-thick fcc Au(100) buffer layers.[17] The Fe film was overcoated with a 20-Å-thick Au(100) layer. The pressure of the MBE chamber was in the 10^{-10} Torr range during deposition. The thicknesses of the films were determined using a quartz thickness monitor. The reflection high-energy electron diffraction pattern showed that the Fe film was single crystalline.

The MCD experiment was performed in the 40–80-eV region using off-plane circularly polarized synchrotron radiation (CPSR) on bending-magnet beamline BL-11D at the Photon Factory, National Laboratory for High Energy Physics. The degree of circular polarization ($|P_C|$) was 75–85 % in the energy region of the present experiment.[18] The measurements were made with a reflection method in the Faraday configuration[12] using an ultrahigh-vacuum-compatible superconducting magnet.[19] The polarization state of the incident beam was fixed in a left-handed CPSR mode, and the direction of the magnetic field (±3 T) was reversed. The light reflected from the sample was detected by a sodium-salicylate-coated photomultiplier, which was specially designed for use under high magnetic fields. In order to obtain the diagonal and off-diagonal dielectric tensor elements through Kramers-Kronig (KK) analyses, we measured the reflectivity in a lower energy region from 4 to 40 eV using a Seya-Namioka monochromator on beamline BL-11C.

The experimental results are shown in Fig. 1. The dotted curves in Figs. 1(a)–1(d) display the reflection MCD (RMCD) spectra, $\Delta R/R=(R_+-R_-)/[(R_++R_-)/2]$, of a single-crystal Fe film, an annealed $Fe_{51}Pt_{49}$ alloy film, an as-deposited $Fe_{51}Pt_{49}$ alloy film, and an Fe/Pt multilayer, respectively. The reflectivity spectra, $R=(R_++R_-)/2$, are also shown by the solid curves in Fig. 1. Here, R_+ and R_- represent the reflectivities involving optical transitions with $\Delta J_z=+1(\sigma_+)$ and $\Delta J_z=-1(\sigma_-)$ with the z axis taken in the direction opposite to the sample magnetization. A correction for P_C was made in the RMCD spectra using an average value of $|P_C|=80\%$.[12,18] The RMCD spectrum of the Fe film exhibits both a lower lying negative peak and a higher lying weaker positive peak at the Fe $M_{2,3}$ core edges. In contrast, the RMCD spectra of the alloys and the multilayer show a strong negative peak at the Fe $M_{2,3}$ edges with almost no positive signal on the high-energy side. The R spectra of the alloys and multilayer exhibit structures arising from the spin-orbit split Pt N_6 (~75 eV) and N_7 (~72 eV) core edges. Strong RMCD signals were observed at the Pt N_6 and N_7 edges for the alloys and multilayer. This clearly demonstrates

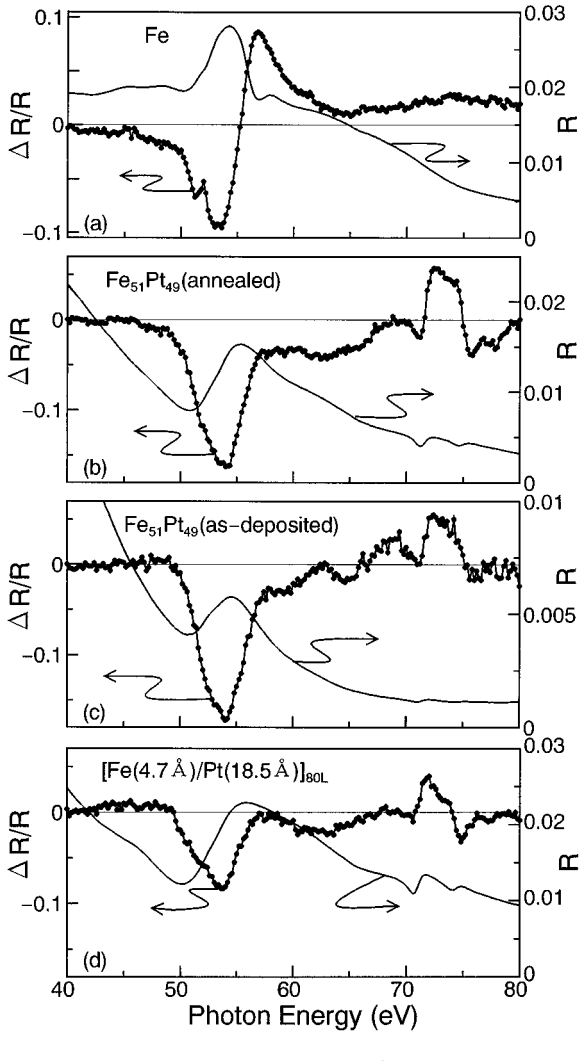

FIG. 1. Reflection MCD spectrum $\Delta R/R=(R_+-R_-)/[(R_++R_-)/2]$ (dotted curves) and reflectivity spectrum R (solid curves). Corrections for the overlayer effects have not yet been made. (a) Single-crystalline Fe film. (b) Annealed $Fe_{51}Pt_{49}$ alloy film. (c) As-deposited $Fe_{51}Pt_{49}$ alloy film. (d) Fe(4.7 Å)/Pt(18.5 Å) multilayer.

that magnetic moments have been induced on Pt atoms in the alloys and multilayer due to hybridization between the Fe $3d$ and Pt $5d$ states.

Both the optical and magneto-optical behavior of solids should be interpreted in terms of the complex dielectric tensor, $\tilde{\epsilon}$.[20] The imaginary part of the diagonal element ϵ_0'' represents usual optical absorption, while that of the off-diagonal element ϵ_1'' represents MCD effects in absorption. Usually, ϵ_0'' and ϵ_1'' can be evaluated directly from measured R and RMCD spectra using the KK transformation and related equations. In the present case, however, it is essential to take into account the influence of the oxidation-prevention overlayer (Au or Pt) on both the R and RMCD spectra.

In order to remove the overlayer effects from the raw data of R and RMCD, we consider the optical and magneto-optical response of a vacuum (medium 1)-overlayer (medium 2)-sample (medium 3) system. The complex reflectivity amplitude for normal incidence of such a system, $\hat{r}$, is given by[21]

$$\hat{r}=\frac{\hat{r}_{12}(\hat{r}_{12}\hat{r}_{13}-1)+(\hat{r}_{12}-\hat{r}_{13})e^{2i\Psi}}{(\hat{r}_{12}\hat{r}_{13}-1)+\hat{r}_{12}(\hat{r}_{12}-\hat{r}_{13})e^{2i\Psi}}, \tag{1}$$

where $\hat{r}_{ij}$ is the complex reflectivity amplitude at the interface between medium i and medium j, and $\Psi = (2\pi/\lambda)\hat{N}_2 d_2$ with λ, $\hat{N}_2$, and d_2 being the wavelength of light, the complex refractive index of medium 2, and the thickness of medium 2, respectively. A KK analysis of the measured R will yield a phase shift on reflection, θ, and hence $\hat{r} = \sqrt{R}e^{i\theta}$. Thus solving Eq. (1) for $\hat{r}_{13} = \sqrt{R_{13}}e^{i\theta_{13}}$ gives the optical constants of medium 3, n_3 and k_3, also yielding $\epsilon_0''(\equiv \epsilon_{0,13}'') = 2n_3k_3$. By taking a logarithmic difference of Eq. (1) for left (σ_+) and right (σ_-) circular polarization, we obtain

$$\frac{\Delta\hat{r}_{13}}{\hat{r}_{13}} \simeq \frac{\Delta\hat{r}}{\hat{r}}\left[1 + \frac{\hat{r}\hat{r}_{12}(1-e^{2i\Psi})}{\hat{r}_{12}(\hat{r}_{12}-\hat{r}) - (1-\hat{r}\hat{r}_{12})e^{2i\Psi}} - \frac{\hat{r}_{12}(1-e^{2i\Psi})}{(\hat{r}_{12}-\hat{r}) - \hat{r}_{12}(1-\hat{r}\hat{r}_{12})e^{2i\Psi}}\right], \quad (2)$$

where $\Delta\hat{r}_{13} = \hat{r}_{13}^{+} - \hat{r}_{13}^{-}$ and $\Delta\hat{r} = \hat{r}^{+} - \hat{r}^{-}$. A KK analysis of the measured $\Delta R/R$ spectrum will give a difference between the phase shifts for left (θ^+) and right (θ^-) circular polarization, $\Delta\theta = \theta^+ - \theta^-$, and hence $\Delta\hat{r}/\hat{r} = \frac{1}{2}\Delta R/R + i\Delta\theta$. Equation (2) thus yields $\Delta\hat{r}_{13}/\hat{r}_{13} = \frac{1}{2}\Delta R_{13}/R_{13} + i\Delta\theta_{13}$, where $\Delta R_{13} = R_{13}^{+} - R_{13}^{-}$ and $\Delta\theta_{13} = \theta_{13}^{+} - \theta_{13}^{-}$. The imaginary part of the off-diagonal tensor element of medium 3, $\epsilon_1''(\equiv \epsilon_{1,13}'')$, is given by

$$\epsilon_1'' = \frac{1}{4}\beta_3\frac{\Delta R_{13}}{R_{13}} + \frac{1}{2}\alpha_3\Delta\theta_{13}, \quad (3)$$

where $\alpha_3 = n_3(n_3^2 - 3k_3^2 - 1)$ and $\beta_3 = k_3(3n_3^2 - k_3^2 - 1)$.

KK analyses were made of the measured R spectra with extrapolation to lower and higher energies. The R below 4 eV was assumed to be that of a free-electron gas. Above 80 eV, the R spectra were extrapolated proportionally to ω^{-4}. Since the RMCD signals are almost zero at the lower and higher limits of the present MCD measurements, no extrapolation to outer regions was made for the KK analyses of the RMCD spectra. The optical constants of Au and Pt reported in the literature[22] were used to evaluate $\hat{r}_{12}$.

The results of the data analyses are shown in Fig. 2. The dotted curves in Figs. 2(a)–2(d) display the ϵ_1'' for an Fe film, an annealed Fe-Pt alloy film, an as-deposited Fe-Pt alloy film, and an Fe/Pt multilayer, respectively. The ϵ_0'' is shown by the solid curves in Fig. 2. A comparison of the $\Delta R/R$ spectra with the corresponding ϵ_1'' spectra shows that the general tendency seen in the $\Delta R/R$ carries over in the ϵ_1''. In order to see the MCD at the Pt $N_{6,7}$ edges more closely, we present the ϵ_1'' spectra at around the Pt $N_{6,7}$ and O_2 edges of the alloys and the multilayer on an expanded scale in Fig. 3. Besides the main MCD signals, fine MCD features were observed and are labeled D and S.

A recently discovered MCD orbital sum rule[23] shows that the integrated intensity of an MCD spectrum over the $L_{2,3}$ or $M_{2,3}$ edges of $3d$ transition metals is directly proportional to the $3d$ orbital moment in the ground state. The presence of the negative and positive peaks in the ϵ_1'' spectrum around the Fe $M_{2,3}$ edges of the Fe film [Fig. 2(a)] results in a substantial cancellation of an integrated MCD intensity. This indicates that the $3d$ orbital moment is small in Fe metal. In contrast, the ϵ_1'' spectra of the alloys [Figs. 2(b) and 2(c)] and the multilayer [Fig. 2(d)] exhibit only a negative peak at the Fe $M_{2,3}$ edges. This finding unambiguously reveals that the

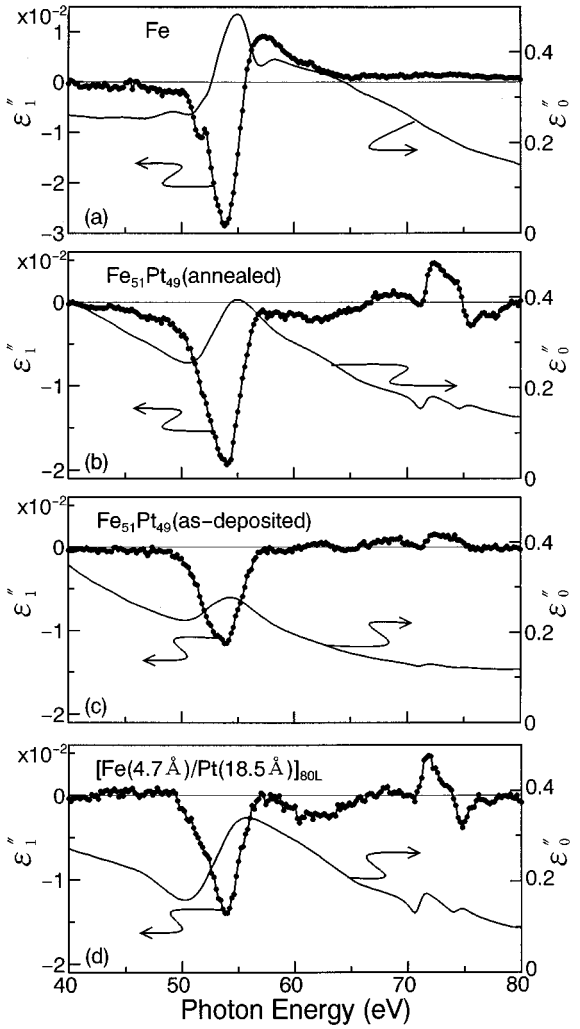

FIG. 2. Imaginary part of the off-diagonal dielectric tensor element ϵ_1'' (dotted curves) and imaginary part of the diagonal dielectric tensor element ϵ_0'' (solid curves). Both ϵ_0'' and ϵ_1'' have been deduced from R and $\Delta R/R$ through Kramers-Kronig analyses with corrections for the effects of the overlayer on R and $\Delta R/R$. (a) Single-crystalline Fe film. (b) Annealed $Fe_{51}Pt_{49}$ alloy film. (c) As-deposited $Fe_{51}Pt_{49}$ alloy film. (d) Fe(4.7 Å)/Pt(18.5 Å) multilayer.

$3d$ orbital moment of Fe is greatly enhanced in the alloys and the multilayer compared with that in Fe metal. This result is in agreement with a recent theoretical calculation,[9] and is also consistent with a recent MCD study at the Co $L_{2,3}$ edges in Co/Pd multilayers.[13]

The ϵ_1'' spectra of the alloys and multilayer are seen to exhibit a very weak positive feature at ~67–68 eV for the Pt O_2 edge (Fig. 3). This leads us to expect a weak negative MCD for the Pt O_3 edge (~52 eV), which merges into the strong Fe $M_{2,3}$ MCD. This MCD sign at the Pt $O_{2,3}$ edges indicates that the induced Pt $5d$ moment is aligned parallel to the Fe $3d$ moment.

Since no studies have been reported to date for MCD associated with transitions involving the $4f_{5/2,7/2}$ initial core states, we consider here the expected MCD at the Pt $N_{6,7}$ edges. Electronic-structure calculations[7,8] show that the unoccupied Pt $5d$ states are predominantly of minority spin, except for those just above the Fermi level (E_F). Thus, we first consider the transitions for the minority spin states. An application of the dipole selection rules with the $5d$ spin-orbit interaction (i.e., $5d$ orbital moment) being taken into

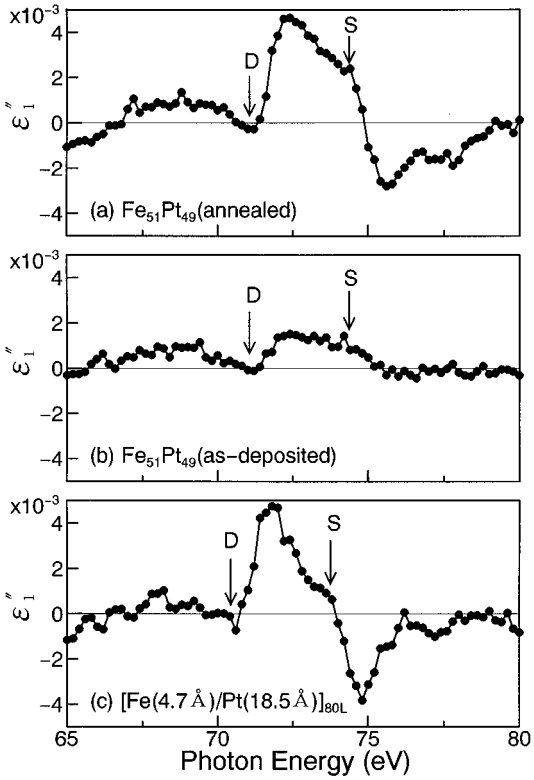

FIG. 3. Imaginary part of the off-diagonal dielectric tensor element ϵ_1'' around the Pt $N_{6,7}$ and O_2 edges. Fine MCD features are labeled *D* and *S*. (a) Annealed $Fe_{51}Pt_{49}$ alloy film. (b) As-deposited $Fe_{51}Pt_{49}$ alloy film. (c)Fe(4.7 Å)/Pt(18.5 Å) multilayer.

account leads to the result that the MCD is positive at the lower-energy N_7 edge, and is negative at the higher-energy N_6 edge. This MCD pattern is opposite to that at the Fe $M_{2,3}$ and Pt $O_{2,3}$ edges if the same quantization axis is taken both for the Fe and Pt total moments. It is noted that the sign of MCD at the Pt $N_{6,7}$ edges is reversed for transitions to the unoccupied majority-spin states.

The ϵ_1'' spectra of the annealed alloy [Fig. 3(a)] and the multilayer [Fig. 3(c)] exhibit a strong positive peak at the Pt N_7 edge and a clear negative peak at the N_6 edge; the MCD is opposite in sign to that at the Fe $M_{2,3}$ and Pt $O_{2,3}$ edges. Although both features in the ϵ_1'' spectrum are much weaker for the as-deposited alloy [Fig. 3(b)], the MCD sign at the Pt $N_{6,7}$ edges is the same as that for the annealed alloy and the multilayer. This result gives clear evidence that the induced Pt total moment is aligned *parallel* to the Fe total moment in the $Fe_{51}Pt_{49}$ alloys and the Fe/Pt multilayer. The present conclusion is inconsistent with the assumption of an antiparallel alignment of the Fe and Pt total moments in the $Fe_{50}Pt_{50}$ ordered alloy, which was deduced from a previous neutron-scattering experiment.[5] On the other hand, our conclusion agrees with the indication of a parallel alignment, obtained from both recent core-level MCD (Refs. 15 and 16) and spin-resolved photoemission[6] measurements.

Figure 3 shows the presence of a dip (*D*) just below the positive MCD peak at the N_7 edge and a shoulder (*S*) just below the negative MCD peak at the N_6 edge in the alloys and the multilayer. These features could be attributed to the MCD associated with transitions to the unoccupied majority-spin states just above E_F. This indicates that the unoccupied majority-spin states have a higher density of states just above E_F than do the unoccupied minority-spin states in the alloys and the multilayer. The present result is in good agreement with the electronic-structure calculation by Podgórny.[8]

In conclusion, we have presented evidence for an enhanced $3d$ orbital moment in Fe-Pt alloys and an Fe/Pt multilayer compared to that in Fe metal and for a ferromagnetic coupling of the Fe and Pt total moments in the alloys and multilayer. Information was obtained concerning the Pt $5d$ partial density of states just above E_F.

The authors thank Professor H. Sugawara, the Director General of National Laboratory for High Energy Physics, for financial support and encouragement. We also thank the staff of the Photon Factory for machine operation.

*Present address: Department of Functional Materials Science, Saitama University, Urawa, Saitama 338, Japan.
†Present address: Personal Systems Laboratories, Fujitsu Laboratories Ltd., Akashi, Hyogo 674, Japan.
‡Present address: National Institute for Advanced Interdisciplinary Research, Tsukuba, Ibaraki 305, Japan.

[1] P. F. Carcia *et al.*, Appl. Phys. Lett. **47**, 178 (1985).
[2] T. Sugimoto *et al.*, Jpn. J. Appl. Phys. **28**, L2333 (1989); J. Magn. Magn. Mater. **104-107**, 1845 (1992).
[3] T. Katayama *et al.*, J. Magn. Magn. Mater. **104-107**, 1002 (1992).
[4] T. Sugimoto *et al.*, Phys. Rev. B **48**, 16 432 (1993).
[5] A. Z. Men'shikov *et al.*, Fiz. Met. Metalloved. **38**, 505 (1974).
[6] M. Finazzi *et al.*, Phys. Rev. B **50**, 14 671 (1994).
[7] V. I. Anisimov and M. A. Korotin, Fiz. Met. Metalloved. **68**, 474 (1989).
[8] M. Podgórny, Phys. Rev. B **43**, 11 300 (1991).
[9] G. H. O. Daalderop *et al.*, Phys. Rev. B **44**, 12 054 (1991).
[10] G. Schütz *et al.*, Phys. Rev. Lett. **58**, 737 (1987).
[11] C. T. Chen *et al.*, Phys. Rev. B **42**, 7262 (1990).
[12] T. Koide *et al.*, Phys. Rev. B **44**, 4697 (1991).
[13] Y. Wu *et al.*, Phys. Rev. Lett. **69**, 2307 (1992).
[14] D. Weller *et al.*, Phys. Rev. B **49**, 12 888 (1994).
[15] G. Schütz *et al.*, J. Appl. Phys. **67**, 4456 (1990).
[16] H. Maruyama *et al.*, Jpn. J. Appl. Phys. Suppl. **32-2**, 290 (1993).
[17] Y. Suzuki *et al.*, Phys. Rev. Lett. **68**, 3355 (1992).
[18] T. Koide *et al.*, Nucl. Instrum. Methods Phys. Res. Sect. A **308**, 635 (1991); Rev. Sci. Instrum. **63**, 1458 (1992).
[19] T. Koide *et al.*, Rev. Sci. Instrum. **63**, 1462 (1992).
[20] For an isotropic or cubic material under a magnetic field along the *z* direction, we define $\tilde{\epsilon}$ as

$$\tilde{\epsilon}=\begin{pmatrix} \epsilon_0 & i\epsilon_1 & 0 \\ -i\epsilon_1 & \epsilon_0 & 0 \\ 0 & 0 & \epsilon_z \end{pmatrix},$$

where $\epsilon_0=\epsilon_0'+i\epsilon_0''$ and $\epsilon_1=\epsilon_1'+i\epsilon_1''$.
[21] L. D. Landau and E. M. Lifshitz, *Electrodynamics of Continuous Media* (Pergamon, Oxford, 1960), p. 278. Landau and Lifshitz give the well-known formula, $\hat{r}=(\hat{r}_{12}+\hat{r}_{23}e^{2i\Psi})/(1+\hat{r}_{12}\hat{r}_{23}e^{2i\Psi})$, together with a particular equation, $\hat{r}_{23}=(\hat{r}_{12}-\hat{r}_{13})/(\hat{r}_{12}\hat{r}_{13}-1)$, which is obtained from the above formula by setting $\hat{r}=\hat{r}_{13}$ for $d_2=0$. Combining these two equations yields Eq. (1) in the text.
[22] *Handbook of Optical Constants of Solids*, edited by E. D. Palik (Academic, Orlando, 1985), p. 286 and p. 333.
[23] B. T. Thole *et al.*, Phys. Rev. Lett. **68**, 1943 (1992).